

Raman spectroelectrochemical study of redox dye Nile blue adsorbed or electropolymerised at a gold electrode

Regina Mažeikienė,
Gediminas Niaura,
Olegas Eicher-Lorka,
Albertas Malinauskas*

*Department of Organic Chemistry,
Center for Physical Sciences
and Technology,
3 Saulėtekio Avenue,
10257 Vilnius, Lithuania*

The redox dye Nile blue has been adsorbed and electrochemically polymerised at a roughened gold electrode. The resulting modified electrodes were subjected to Raman spectroelectrochemical study with 785 nm laser line excitation. For both types of electrodes, well-expressed and rich in features Raman spectra were obtained. The spectra are closely related to those of another oxazine type redox dye Meldola blue. At solution pH 7.0, the overall intensity of the Raman spectra for both types of modified electrodes appears higher than in a pH 1.0 solution. Probably, this is caused by different light absorbance properties of this dye in two solutions. In a pH-neutral solution, the dye possess light absorbance in the red range of the visible spectrum, thus, resonance enhancement is possible. The intensity of the Raman spectra also increases by the shift of the electrode potential to higher positive values. This effect could be understood taking into account an intensifying colouration of the dye at a stepwise increase of the electrode potential due to a continuous growth of the content of oxidised forms within the electrode-bound layer.

Keywords: Raman spectroscopy, spectroelectrochemistry, redox mediators, Nile blue

INTRODUCTION

The redox dye Nile blue (NB) has been extensively used during several decades in different electrochemistry-related applications as a suitable electron mediator. Nowadays, the research interest in its useful properties and possible applications continues to grow with introduction of new electroanalytical techniques, new modern materials, and new application ideas. Many works relate to analytical applications of this redox dye. A complex composite electrode consisting of re-

duced graphene oxide, gold nanoparticles and NB has been proposed as a sensitive probe for electrochemical dopamine detection [1]. NB has been used in creating of a nanosandwich device containing a graphene oxide thin film for electrochemical in vivo monitoring of interleukin-6 [2]. Based on a combination of electrochemical and surface enhanced Raman scattering techniques, a sandwich-type immunoassay for the detection of a carcinoembryonic antigen has been developed with the use of NB as a Raman probe [3]. The development of multiplexed electrochemical biosensors with the use of NB and other redox mediators was described [4]. Electrocatalytic activity

* Corresponding author. Email: albertas.malinauskas@ftmc.lt

and possible applications to electrochemical detection of hydrogen peroxide and nitrite anion has been described for graphene nanosheets and NB nanocomposite [5]. Reduced graphene oxide and NB nanocomposites were proposed for an electrochemical label-free immunosensor for carcinoembryonic antigen detection [6]. A glassy carbon electrode containing a layer of electropolymerised NB was used for voltammetric detection of important bioanalytes like paracetamol and caffeine [7]. With the use of a specially prepared pencil graphite electrode and NB as an electroactive indicator, an electrochemical DNA sensor for detection of hepatitis virus was reported [8].

Next to electroanalytical applications, some different fields for the use of NB were proposed. NB has been quite popular as a redox Raman active probe in creating of different modifications of Raman spectroscopy. Covalently tethered to a gold electrode NB has been tested using in situ tip-enhanced Raman spectroscopy (TERS), and a reversible decrease of TERS intensity was found upon electrochemical reduction of NB [9]. Similarly, a combination of TERS with atomic force microscopy and electrochemistry has been used to observe the nanoscale spacial distribution of a formal potential with the use of single molecule NB spectroelectrochemistry spaced at 5–10 nm from the electrode [10]. A number of other applications of this redox dye related to micro- and nanoelectrochemistry [11–13], or to specific problems of electrocatalysis [14, 15] have been reported.

For successful applications of NB in different fields, a deep knowledge on its spectroelectrochemical properties appears an important prerequisite. In our preceding works, we performed detailed Raman spectroelectrochemical studies on related redox mediators used in electrochemical systems – toluidine blue [16], neutral red [17] and Meldola blue [18]. In order to broaden our studies to other redox mediators and dyes, in the present study we aimed at Raman spectroelectrochemical investigation of the redox dye Nile blue, adsorbed and electrochemically polymerised at a gold electrode.

EXPERIMENTAL

Nile blue (IUPAC name: [9-(diethylamino)benzo[*a*]phenoxazin-5-ylidene]azanium sulfate,

NB, Sigma) and other chemicals were used as received. A BASi Epsilon model potentiostat (Bioanalytical Systems Inc., USA) was used throughout the experiments. A flat circular gold electrode of ca. 5 mm in diameter, press-fitted into a Teflon rod, as a working electrode, a platinum wire as a counter electrode, and a KCl saturated Ag/AgCl reference electrode were used throughout the work. All potential values reported below refer to this reference electrode. Before each experimental set, the working electrode has been cleaned for 1 h in a Piranha solution (a mixture of 30% hydrogen peroxide and concentrated sulfuric acid, 3:1 by vol.), and ultrasonicated for 2 min in an ethanol and water mixture. Then, the surface of a gold electrode was electrochemically roughened for the Raman experiment by potential cycling for 50 cycles in a 0.1 M KCl solution within an electrode potential window of –0.3 to 1.4 V at a potential scan rate of 200 mV/s.

The electrode was modified with Nile blue by adsorbing the dye from its 1 mM solution in a 0.01 M phosphate buffer solution pH 6.9, containing 0.1 M of sodium sulfate, for 1 h. Electropolymerisation of NB was performed by potential cycling within the limits of –0.6 to 1.0 V for 10 cycles at a scan rate of 100 mV/s in an above-mentioned solution. After the electropolymerisation, the electrode was rinsed in a supporting electrolyte, and mounted into an electrochemical or spectroelectrochemical cell. Phosphate buffer solutions pH 7.0, containing additionally 0.1 M of sodium sulfate, or the 0.1 M solution of sulfuric acid pH 1.0, were used as supporting electrolytes for experiments, as indicated in the text.

Raman spectroelectrochemical experiments were performed in a cylinder-shaped three electrodes moving spectroelectrochemical cell, arranged with a gold working electrode (as described above), a platinum wire counter electrode, and a KCl saturated Ag/AgCl reference electrode. SERS spectra were recorded using an Echelle type spectrometer RamanFlex 400 (PerkinElmer, Inc.) equipped with a thermoelectrically cooled (–50°C) CCD camera and a fiber-optic cable for excitation and collection of the Raman spectra. The 785-nm beam of the diode laser was used as the excitation source. The 180° scattering geometry was employed. The laser power at the sample was restricted to 10 mW and the beam was

focused to a 200 μm diameter spot on the electrode. The integration time was 10 s. Each spectrum was recorded by accumulation of 10 scans yielding the overall integration time of 100 s. The Raman frequencies were calibrated using the polystyrene standard (ASTM E 1840) spectrum. No smoothing procedures were applied to the experimental data. The working electrode was placed at approx. 3 mm distance from the cell window. In order to reduce photo- and thermo-effects, and a possible degradation of an adsorbate or a polymer film by the incident light as well, the cell holder was moved periodically with respect to the laser beam at ca. 15–25 mm/s with the help of custom-built equipment [19].

RESULTS AND DISCUSSION

Figure 1 shows the molecular structure of Nile blue (NB) in its oxidised and protonated form. For

comparison, its similar structural analogue Meldola blue is also depicted. The only difference of the latter is the absence of a primary amino group at the ring. Both dyes possess electrochemical redox activity and thus are used as redox mediators especially for biosensors. Figure 2 illustrates cyclic voltammograms for NB as obtained at a gold electrode for an extended anodic scan. In the first anodic potential scan, NB shows a clear oxidation peak centered at -0.25 V, and a high anodic current at a high positive potential exceeding 0.8 V. In the back cathodic scan, a clear reduction wave around -0.35 V is observed. From this, the midpoint redox potential for NB of about -0.30 V could be derived for the particular conditions used. For NB, the formal potentials of 0.406 and -0.119 V (vs NHE) for the solution pH of 0.0 and 7.0, respectively, were reported [20]. For NB embedded into a self-assembled thiol layer at a gold electrode, a formal potential of -0.387 V vs SCE

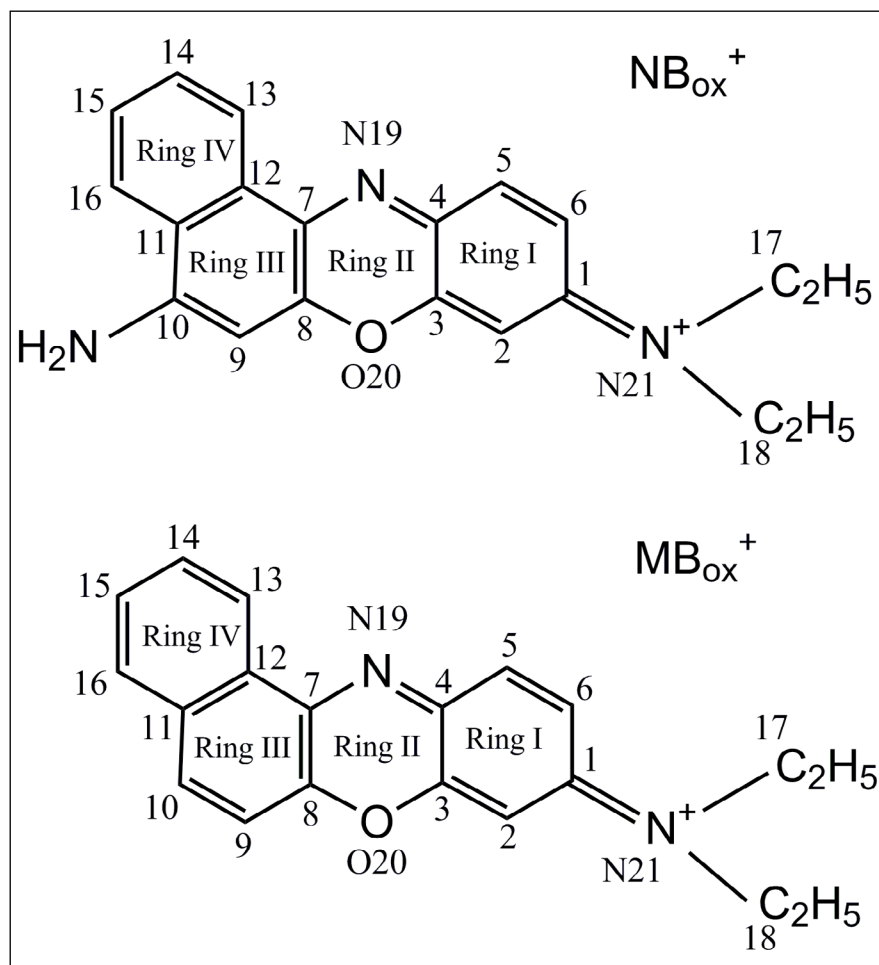


Fig. 1. Atom and ring numbering for oxidised protonated forms of Nile blue (at the top) and Meldola blue (at the bottom)

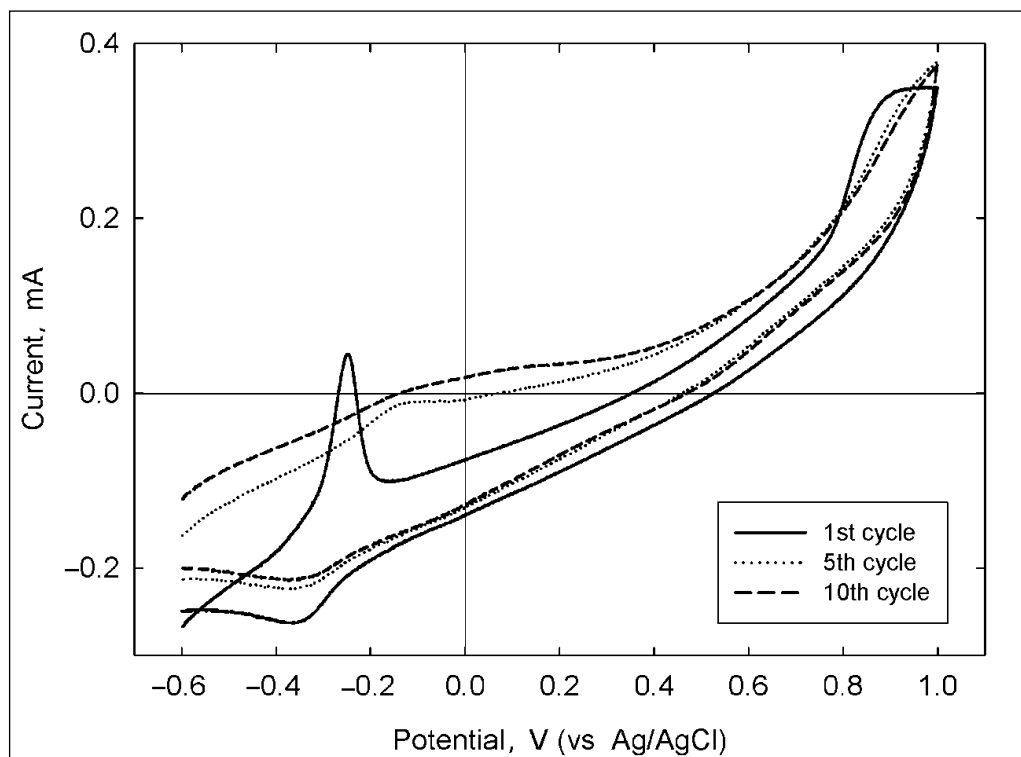


Fig. 2. Cyclic voltammograms for the gold electrode, as obtained for the 1st, 5th and 10th potential scan (as indicated) within scan limits of -0.6 to 1.0 V at a scan rate of 100 mV/s in a solution containing 1 mM of Nile blue, 0.1 M Na_2SO_4 , 0.01 M Na_2HPO_4 and 0.01 M NaH_2PO_4

in the pH 5.5 phosphate buffer solution has been reported [21]. At the electrode potential exceeding 0.7 – 0.8 V, a high anodic current is observed, indicating probably the irreversible oxidation of NB to reactive radical species to proceed. By repeating potential scans, both anodic and cathodic peaks become less pronounced, although the redox capacity grows up, as it could be deduced from increasing charge passed during continuing potential cycling (Fig. 2). In the first few potential scans, an anodic peak for NB slightly shifts to less negative values (e.g. up to -0.13 V in the 5th consecutive scan), whereas the cathodic peak does not change its position around -0.35 V. At a prolonged potential scan, a broadened anodic peak is observed (Fig. 2). In a common sense, this electropolymerisation process appears quite similar to that of other related azine type redox dyes like toluidine blue [16], neutral red [17], or Meldola blue [18].

After a prolonged potential cycling, a stable layer of electropolymerised NB appears at the electrode surface. When transferred into a solution not containing a NB monomer, the poly(Nile blue) (PNB) modified electrode shows a pair of anodic

and cathodic peaks typical for this redox couple. Figure 3 shows cyclic voltammograms for PNB modified electrodes, and gold electrodes containing adsorbed but not electropolymerised NB, in acidic and neutral solutions. At the solution pH of 1.0 , both types of the modified electrode show anodic peaks around 0.12 V along with their cathodic counterparts around 0.00 V, yielding thus a midpoint value of 0.06 V. In the pH 7.0 solution, the electrode modified with adsorbed NB shows a pair of cathodic and anodic peaks at a midpoint potential of -0.30 V and ΔE_p of 0.21 V. The PNB modified electrode shows a cathodic peak around -0.35 V, and a flat anodic counterpart within a broad potential range (Fig. 3). A related value for the midpoint potential of PNB prepared at a glassy carbon electrode of -0.41 V vs SCE has been reported for the pH 7.0 phosphate buffer solution [22].

For the oxidised form of NB, a pK value of 9.70 was reported, whereas the reduced form possesses two protonation steps with pK values of 3.92 and 6.90 [20]. This means that in both solutions used, pH 1.0 and pH 7.0 , the oxidised form of NB appears protonated via a primary amino group in

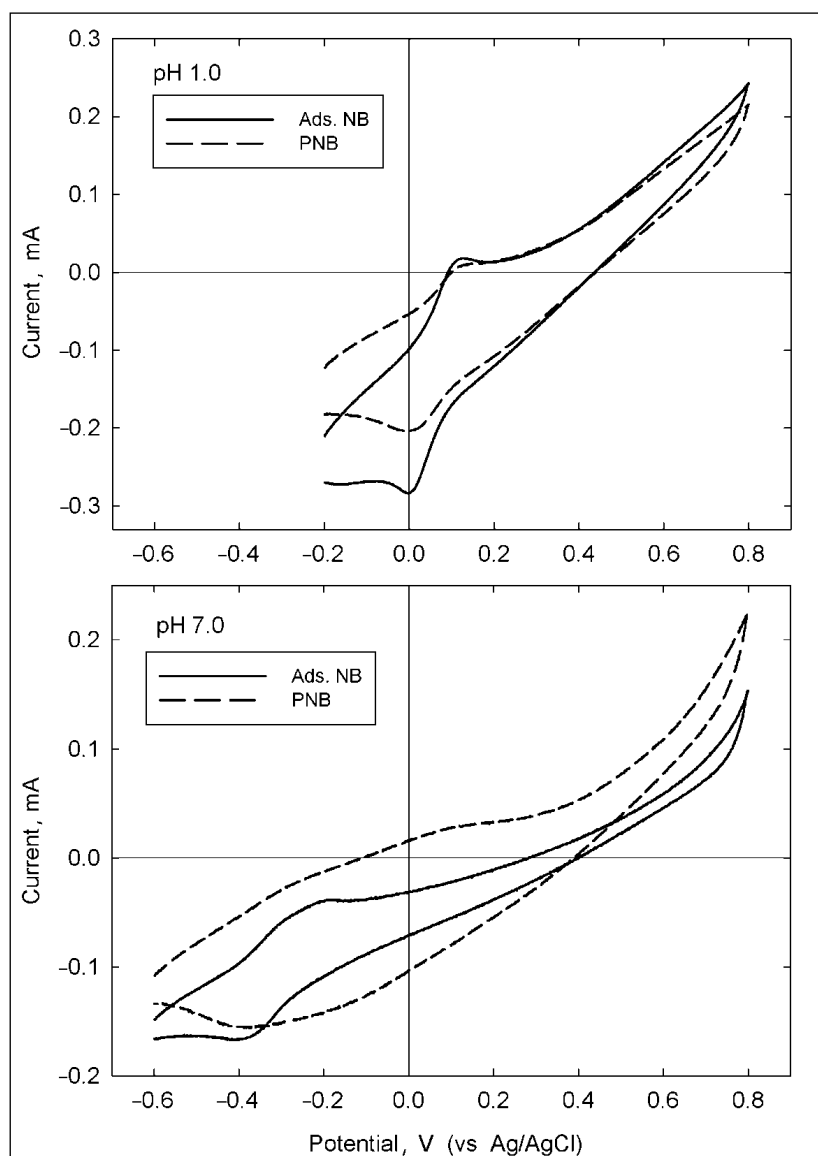


Fig. 3. Cyclic voltammograms for the gold electrode with adsorbed Nile blue (Ads. NB) and polymerized Nile blue (PNB, as indicated), as obtained in the pH 1.0 solution containing 0.1 M H_2SO_4 (at the top), or the pH 7.0 solution containing 0.1 M Na_2SO_4 , 0.01 M Na_2HPO_4 , and 0.01 M NaH_2PO_4 (at the bottom) at a scan rate of 100 mV/s within the limits of -0.2 to 0.8 V (at the top), or -0.6 to 0.8 V (at the bottom)

its structure (Fig. 1), whereas the reduced form of NB appears protonated in the pH 1.0 solution, and deprotonated at pH 7.0.

Both types of the modified electrodes, containing either electropolymerised or adsorbed layers of NB, were subjected to Raman spectroscopic study with the use of far red laser spectra excitation at 785 nm. The corresponding Raman spectra are presented in Figs. 4 and 5 for the PNB and adsorbed NB electrodes, respectively. As it could be expected, the spectra obtained appear rich in Raman features because of a high number of vibration modes for this structure. Previously, we

obtained somewhat rich in features spectra for related structures like toluidine blue, neutral red and Meldola blue [16–18]. Obviously, all Raman bands observed present combined vibration modes which include many atoms and bonds between them. Previously, we calculated Raman vibrational modes for a similar structural analogue of NB, redox dye Meldola blue [18]. Table presents a summary of Raman bands for NB along with the analogous bands for Meldola blue, as well as their tentative assignments based on our calculations. It is well seen that both structures possess closely similar Raman features. The differences

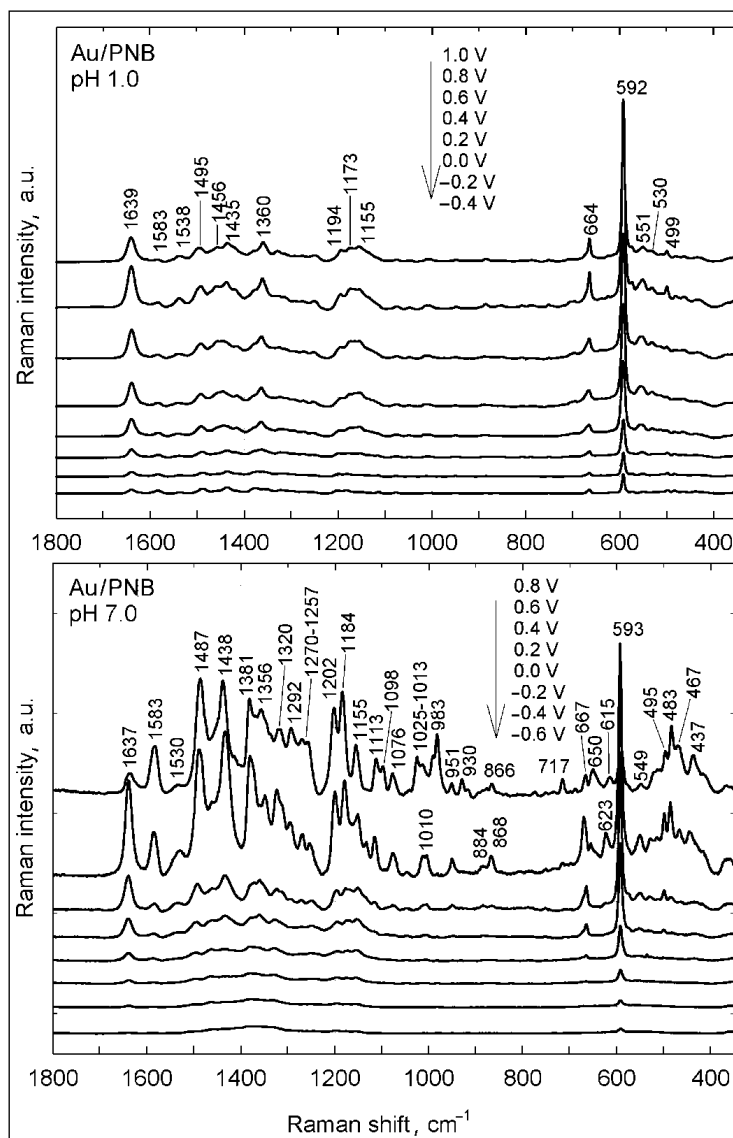


Fig. 4. Raman spectra obtained from the gold electrode with electropolymerised Nile blue at laser excitation wavelength of 785 nm in pH 1.0 (at the top) and pH 7.0 solutions (at the bottom) by stepwise changing the electrode potential from 1.0 to -0.4 V (for pH 1.0 solution) and from 0.8 to -0.6 V (for pH 7.0 solution) by increments of 0.2 V

in frequencies for the most prominent bands for these two related structures are as small as a few cm^{-1} , and the relative intensities for the corresponding bands are also related in values.

It is seen from Figs. 4 and 5 that an overall intensity of spectra appears higher in a pH-neutral than in an acidic solution. Although most Raman bands are observed in both solutions, the most prominent bands appear better expressed in a neutral solution. Also, a few new bands appear when changing the solution acidity to higher pH values like, e.g. the band at $1384\text{--}1381$ cm^{-1} and sharp feature at 983 cm^{-1} visible in the spectrum

obtained at 0.8 V (pH 7.0 solution). The latter band might be associated with the symmetric stretching vibration of SO_4^{2-} ion [23]. In general, the spectrum of PNB obtained at 0.8 V differs from the spectra recorded at a less positive electrode potential. Thus, the spectroscopic data suggest the presence of a different form of a positively charged surface bound polymer able to participate in the ion-pairing process with solution anions. The band from the surface bound SO_4^{2-} anions disappears after switching the potential to less positive values (Fig. 4, bottom). In the aqueous solution, NB shows a strong light absorbance with

Table. Tentative assignments of the Raman bands (their frequencies are given in cm^{-1}) of polymerised and adsorbed Meldola Blue and Nile Blue dyes on the roughened Au electrode at different solution pH values (as indicated)

Raman bands (in cm^{-1})								Tentative assignments
pH 1.0				pH 7.0				
PolyMB	PolyNB	Ads. MB	Ads. NB	PolyMB	PolyNB	Ads. MB	Ads. NB	
1637 s	1639 s	1636 s	1639 s	1631 s	1637 s	1630 s	1639 s	$\nu(\text{C6-C5}) + \nu(\text{C2-C3}) + \nu(\text{C1-N21})$ in-phase [ring-I (C=C) stretching]
1584 w	1583 w	1585 w	1583 w	1576 m	1583 m	1575 m	1584 m	$\nu(\text{C11-C12}) + \nu(\text{C14-C15}) + \nu(\text{C9-C10})$
1551 w	1538 w	1553 w	1538 m	1560 w	1530 w	1560 w	–	$\nu(\text{N21-C1}) + \nu(\text{C2-C3}) +$ $+ \nu(\text{C4-N19}) + \nu(\text{C-C})$ ring-IV
1481 s	1495 m	1482 s	1492 s	1473 s	1487 s	1473 s	1490 s	$\delta(\text{C17H}) + \nu(\text{C4-N19}) + \nu(\text{C1-N21}) + \nu(\text{C2-C3})$
1431 w	1435 w	1430 w	1437 w	1427 s	1438 s	1428 s	1433 s	$\nu(\text{C-C})$ ring-IV + $\nu_s(\text{C4-N19-C7}) +$ $+ \nu(\text{N21-C1}) + \nu(\text{C5-C6})$
–	–	1385 sh	–	1384 s	1381 m	1384 s	1374 m	$\nu(\text{C-C})$ ring-I + $\nu(\text{C7-C12}) + \nu(\text{C4-N19-C7})$
1352 s	1360 s	1352 s	1360 s	1351 vs	1356 m	1351 vs	1345 w	$\nu(\text{C11-C12}) + \nu(\text{C-C})$ ring-IV + $\nu(\text{C1-N21}) + \nu_{as}(\text{C4-N19-C7}) +$ $+ \beta(\text{C5H}) + \beta(\text{C9H})$
1311 w	–	1310 w	–	1311 w	1320 w	1316 sh	1322 w	$\nu_s(\text{C4-N19-C7}) + \beta(\text{CH})$ ring-IV + $\beta(\text{CH})$ ring-III + $\beta(\text{C2H})$
1253 w	–	–	–	–	1292 w	1280 w	1294 w	$\beta(\text{C10H})$ ring-III + $\beta(\text{CH})$ ring-IV + $\nu(\text{C10-C11}) + \nu(\text{C12-C13}) +$ $+ \nu(\text{C4-N19}) + \nu(\text{C1-C2}) + \nu_{as}(\text{C18N21C17})$
1231 m	–	1231 m	1249 m	1233 s	–	1233 s	–	$\beta(\text{CH})$ ring-IV + $\beta(\text{C11-C16}) +$ $+ \beta(\text{C9H}) + \nu(\text{N19-C7})$
1185 s	1194 w	1187 s	1194 m	1182 s	1184 s	1182 s	1200 m	$\beta(\text{CH})$ ring-IV + $\nu_{as}(\text{C4-N19-C7}) +$ $+ \beta(\text{CH})$ ring-I
1152 s	1155 w	1152 s	1152 w	1152 s	1155 m	1151 s	1154 w	$\beta(\text{C6H}) + \beta(\text{C5H})$ ring-I + $\beta(\text{CH})$ ring-IV + $\nu_{as}(\text{C4-N19-C7})$
665 w	–	668 w	664 s	664 w	667 m	664 w	669 m	$\nu_s(\text{C12-C13-C14})$ ip + $\nu_s(\text{C11-C16-C15})$ ip ring-IV + $\nu_{as}(\text{C1-C6-C5})$ ring-I
593 vs	592 s	594 vs	592 vs	596 s	593 s	595 s	592 s	$\nu_s(\text{C3-O20-C8}) + \nu_s(\text{C4-N19-C7})$ [ring-II breathing]
542 m	–	542 m	550 m	540 m	549 w	540 m	549 w	$\delta(\text{C1N21C18C17})$ ip + $\delta(\text{CCC})$ ring-IV ip
500 w	–	500 w	499 w	506 w	495 w	505 w	498 w	$\delta(\text{CCC})$ ring-III ip + $\delta(\text{CCC})$ ring-IV ip + $\delta(\text{C18N21C17})$ ip
463 w	–	469 w	–	469 m	–	469 m	–	$\delta(\text{C1N21C17})$ ip + $\delta(\text{CCC})$ ring-III ip
–	–	439 w	–	447 w	443 w	–	–	$\delta(\text{C18N21C17}) + \delta(\text{CCC})$ ring-IV ip + $\delta(\text{CCC})$ ring-III ip

Abbreviations used: PolyMB: electropolymerized Meldola Blue; PolyNB: electropolymerised Nile Blue; Ads. MB: adsorbed Meldola Blue; Ads. NB: adsorbed Nile Blue; vs: very strong; s: strong; m: middle; w: weak; sh: shoulder; ν : stretching; ν_s : symmetric stretching; ν_{as} : asymmetric stretching; δ : bending; β : in-plane bending; γ : out-of-plane deformation; ip: in-plane. Assignments are based on the analysis of the calculated Raman spectrum for MBOx+ (DFT-B3LYP/6-311+G(2d,p)), presented in [18].

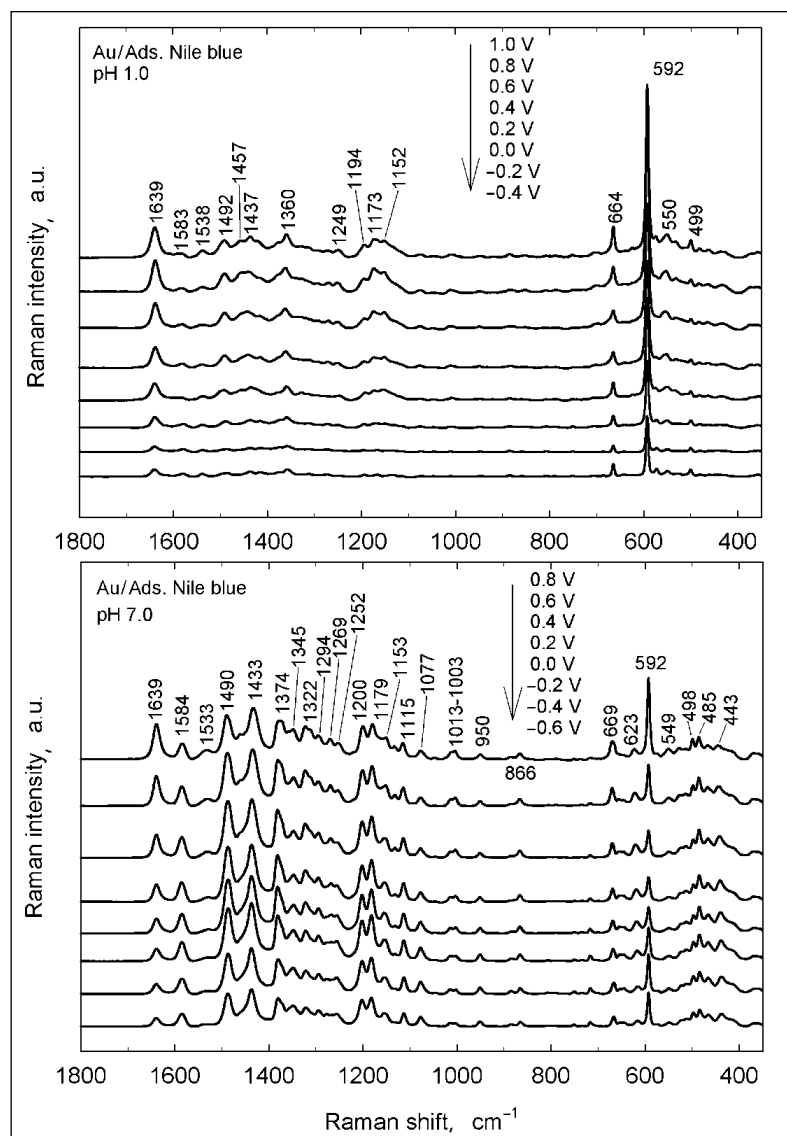


Fig. 5. Same as in Fig. 4, as obtained for the gold electrode containing a layer of adsorbed Nile blue

the band maximum centered at 635 nm, and a shoulder around 590 nm indicating the aggregation of NB molecules [24, 25]. In the solution of 0.1 N HCl (pH 1.0), a new band at shorter wavelengths around 457 nm is observed [24, 25], caused probably by the protonation of NB at low pH values to its dication form [25]. It seems likely that in the pH-neutral solution the Raman spectra excitation laser line of 785 nm falls into a partial resonance with the light absorbance band of NB in the red range of the visible spectrum. In the acidic solution, the absorbance maximum of NB appears blue-shifted by approx. 180 nm, thus avoiding the resonance enhancement. Therefore, the Raman spectra observed in the neutral solution appear of a higher overall intensity.

Another feature of Raman spectra obtained is a higher overall intensity at higher electrode potentials. Figure 6 compares relative intensities for one of the most prominent Raman bands centered at 1639 cm^{-1} for PNB and adsorbed NB as a function of the electrode potential for two solutions used. For PNB, a very low intensity at the lowest potentials is observed in both solutions. The intensity grows progressively by increasing the electrode potential reaching its maximum values at 0.6 or 0.8 V for pH 7.0 and pH 1.0 solutions, respectively (Fig. 6a). At the highest potential values, the intensity drops to some extent. Somewhat different picture is observed for adsorbed dye. Again, an increase of intensity proceeds at a positive potential

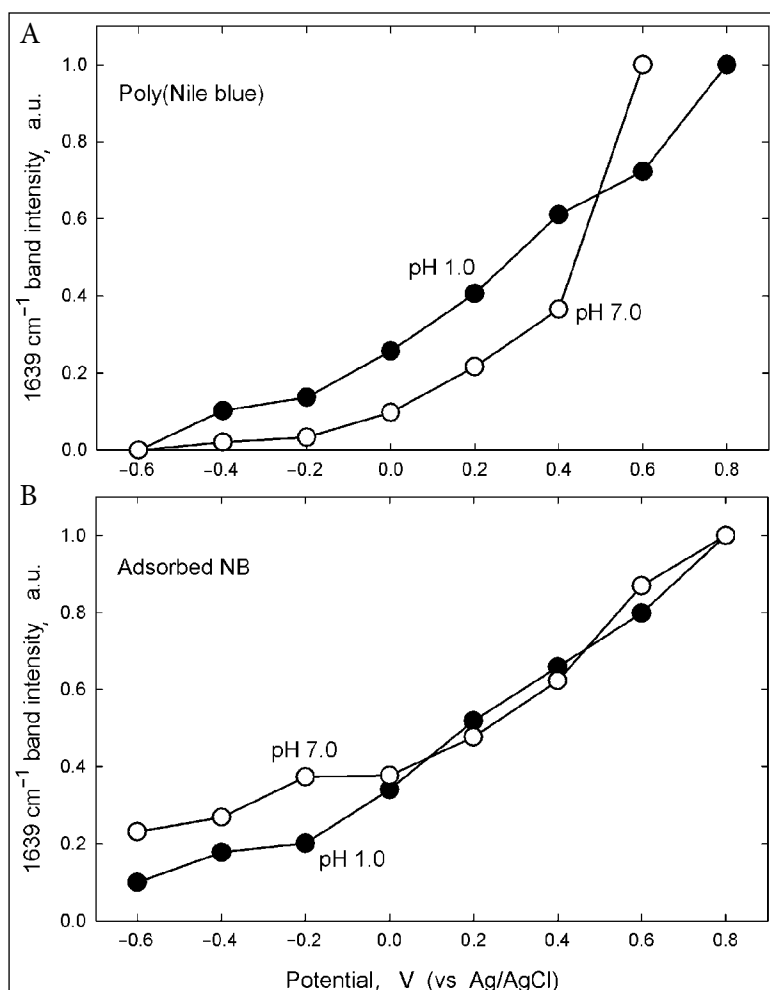


Fig. 6. Dependence of the 1639 cm^{-1} Raman band intensity on the electrode potential for modified electrodes containing PNB (A) or adsorbed NB (B) in pH 1.0 and 7.0 solutions (as indicated)

shift, however, even at the lowest electrode potentials, Raman spectra of a remarkable intensity are observed (Fig. 6b). The most probable reason for this is that some residual part of the adsorbed dye appears not accessible to electrochemical reduction in contrast to the electropolymerised derivative with a more compact and dense structure that allows the electrochemical processes to proceed to a full extent. Apart from changes in intensities, almost no new Raman features are observed by changing of the electrode potential except for some minor changes. Since the electrode potential has been varied under the conditions specified for Figs. 4 and 5 within a very broad range of -0.4 to 1.0 V or -0.6 to 0.8 V for the pH 1.0 and pH 7.0 solutions, respectively, the reversible electrochemical oxidation and reduction of the PNB layer proceeded, as it could be deduced taking into account cyclic voltammograms in

Fig. 3. This means that, except for spectral intensity, no visible qualitative changes in the Raman spectra take place upon electrochemical oxidation and reduction. This seems to be in contrast with our preceding works dealing with Raman spectroelectrochemistry of structurally similar redox dyes, toluidine blue [16] and neutral red [17], but coincides with the studies on Meldola blue [18].

These differences could be well understood taking into account different wavelengths of laser lines used for the excitation of spectra. In the case of toluidine blue, we used a red laser excitation line at 676.4 nm [16]. For the adsorbed layer of this dye at a thin transparent gold electrode, we observed a broad light absorbance band centered at 589 nm [16]. The laser excitation line falls at a shoulder of this broad band, thus, a resonance enhancement of the spectra for the oxidised (blue coloured) form of this dye proceeds. As a result,

both oxidised and reduced forms are clearly distinguishable by corresponding Raman spectra at appropriate electrode potentials and solution pH values. The same applies for neutral red – despite of a somewhat bigger difference between its absorbance maximum and excitation wavelength at 676.4 nm, both redox forms for the electropolymerised and adsorbed dye were well distinguishable [17]. As distinct from both these redox dyes, almost no or only negligible changes in the Raman spectra for the oxidised and reduced forms were observed for Meldola blue [18]. In this case, we used a 785 nm laser line excitation. In the aqueous solution, we found a light absorbance maximum for Meldola blue at 568 nm, whereas a thin layer of the electropolymerised dye at a thin transparent gold electrode showed a remarkable blue shift of the absorbance maximum up to 520 nm [18]. Thus, the spectra excitation wavelength does not coincide or overlap with the optical absorbance band. As a result, no remarkable qualitative differences in the Raman spectra were observed for the oxidised and reduced forms of this redox dye at the appropriate potentials.

In the present case, the situation resembles that of Meldola blue. Although the absorbance maximum falls into the red range of the visible spectrum at 635 nm, it appears far-distanced from the laser line excitation wavelength of 785 nm. Therefore, no enhancement of the Raman spectrum is observed.

CONCLUSIONS

1. When adsorbed or electropolymerised at a gold electrode, the redox dye Nile blue shows numerous Raman features, closely related to those of its oxazine type structural analogue Meldola blue.

2. In a pH-neutral solution, an overall intensity of 785 nm laser line excited Raman spectra appears higher than in an acidic solution, probably because of a resonance enhancement due to different light absorbance properties in the two solutions.

3. The intensity of Raman spectra increases by shifting the electrode potential to higher positive values due to increasing colouration of the dye layer by extending of its net oxidation degree.

References

1. H. Jin, C. Q. Zhao, R. J. Gui, X. H. Gao, Z. H. Wang, *Anal. Chim. Acta*, **1025**, 154 (2018).
2. M. Qi, J. W. Huang, H. Wei, et al., *ACS Appl. Mater. Interfaces*, **9**, 41659 (2017).
3. L. Li, W. B. Lu, C. Liu, Y. Wang, J. Dong, W. P. Qian, *Nano*, **12**, Article No. 1750092 (2017).
4. D. Kang, F. Ricci, R. J. White, K. W. Plaxco, *Anal. Chem.*, **88**, 10452 (2016).
5. R. K. Shervedani, E. Ansarifar, M. S. Foroushani, *Electroanalysis*, **28**, 1957 (2016).
6. Y. S. Gao, X. F. Zhu, J. K. Xu, et al., *Anal. Biochem.*, **500**, 80 (2016).
7. S. Chittravathi, N. Munichandraiah, *J. Electroanal. Chem.*, **764**, 93 (2016).
8. E. Alipour, F. N. Allaf, T. Mahmoudi-Badiki, *J. Solid State Electrochem.*, **20**, 183 (2016).
9. X. Chen, G. Goubert, S. Jiang, R. P. Van Duyne, *J. Phys. Chem. C*, **122**, 11586 (2018).
10. M. Mattei, G. Kang, G. Goubert, et al., *Nano Lett.*, **17**, 590 (2017).
11. A. J. Wilson, N. Y. Molina, K. A. Willets, *J. Phys. Chem. C*, **120**, 21091 (2016).
12. A. J. Wilson, K. A. Willets, *Analyst*, **141**, 5144 (2016).
13. D. Kurouski, M. Mattei, R. P. Van Duyne, *Nano Lett.*, **15**, 7956 (2015).
14. A. A. Ensafi, S. A. S. Afiuni, B. Rezaei, *J. Electroanal. Chem.*, **816**, 160 (2018).
15. R. K. Shervedani, A. Amini, N. M. Sedeh, *Int. J. Hydrogen Energy*, **41**, 13459 (2016).
16. R. Mažeikienė, G. Niaura, O. Eicher-Lorka, A. Malinauskas, *Vibrat. Spectrosc.*, **47**, 105 (2008).
17. R. Mažeikienė, K. Balskus, O. Eicher-Lorka, G. Niaura, R. Meškys, A. Malinauskas, *Vibrat. Spectrosc.*, **51**, 238 (2009).
18. R. Mažeikienė, G. Niaura, O. Eicher-Lorka, A. Malinauskas, *J. Colloid Interface Sci.*, **357**, 189 (2011).
19. G. Niaura, A. K. Gaigalas, V. L. Vilker, *J. Raman Spectrosc.*, **28**, 1009 (1997).
20. J. Ottoway, in: E. Bishop (ed.), *Indicators*, Pergamon, Oxford (1972).
21. H.-H. Liu, J.-L. Lu, M. Zhang, D.-W. Pang, *Anal. Sciences*, **18**, 1339 (2002).
22. R. K. Shervedani, A. Amini, *Electrochim. Acta*, **173**, 354 (2015).
23. G. Niaura, A. Malinauskas, *J. Chem. Soc., Faraday Trans.*, **94**, 2205 (1998).
24. J. Jose, K. Burgess, *Tetrahedron*, **62**, 11021 (2006).
25. M. Krihak, M. T. Murtagh, M. R. Shahriari, *J. Sol-Gel Sci. Technol.*, **10**, 153 (1997).

Regina Mažeikienė, Gediminas Niaura,
Olegas Eicher-Lorka, Albertas Malinauskas

**ADSORBUOTO AR ELEKTROCHEMIŠKAI
POLIMERIZUOTO ANT AUKSO ELEKTRODO
REDOKSO DAŽO NYLO MĒLIO RAMANO
SPEKTROELEKTROCHEMINIS TYRIMAS**

Santrauka

Redokso dažas Nylo mēlis buvo adsorbuotas ir elektrochemiškai polimerizuotas ant aukso elektrodų. Taip paruošti modifikuoti elektrodai buvo tiriami Ramano spektroelektrocheminiu metodu, sužaditimui naudojant 785 nm lazerio spindulį. Abiejų tipų elektrodai buvo paveikti geros kokybės Ramano spektrais, kurie kokybiškai artimi kito redokso dažo Meldola mēlio spektrams. Esant tirpalo pH 7,0, spektrai pasižymi aukštesniu intensyvumu nei esant pH 1,0. Tikėtina, kad tokį skirtumą lemia skirtingos dažo šviesos sugerties savybės šiuose įvairiuose tirpaluose. Ramano spektrų intensyvumas taip pat didėja paslenkant elektrodo potencialą aukštesnių verčių link. Šis reiškinys aiškinamas modifikatoriaus sluoksnio spalvos intensyvėjimu, kuriam įtakos turi oksiduotos formos santykinio kiekio didėjimas.